

# RECONSTRUCTION OF HIGH-RESOLUTION VELOCITY FIELDS IN TURBULENT FLOWS FROM LOW-RESOLUTION MEASUREMENTS

LINH VAN NGUYEN

LML FRE 3723, CRISTAL-CNRS UMR 9189  
UNIVERSITÉ DE LILLE, 59655 VILLENEUVE D'ASCQ

SEPTEMBER 16, 2016

JURY MEMBERS: DR. ETIENNE MÉMIN  
PR. OLIVIER MICHEL  
PR. DANAILA LUMINITA  
PR. NICOLAS DOBIGEON

SUPERVISORS: DR. JEAN-PHILIPPE LAVAL  
DR. PIERRE CHAINAIS



Laboratoire  
Mécanique  
Lille

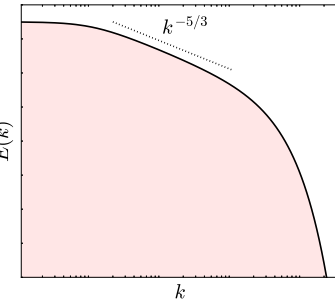
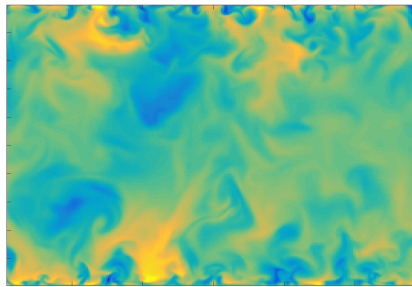


Région  
**Hauts-de-France**  
Nord Pas de Calais - Picardie

- 1 Problem definition
  - Context of the present work
  - The two addressed problems
  - Datasets for numerical experiments
- 2 The proposed approaches
  - Related approaches
  - Mapping functions between large and small scales
  - Fusion of complementary measurements
- 3 Analyses of models performances
  - On isotropic turbulence dataset
  - On turbulent channel flow dataset
- 4 Conclusions and perspectives
  - Conclusions
  - Suggestions for future works
  - Contributions

# Turbulence is multiscale

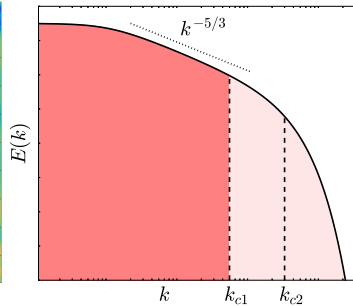
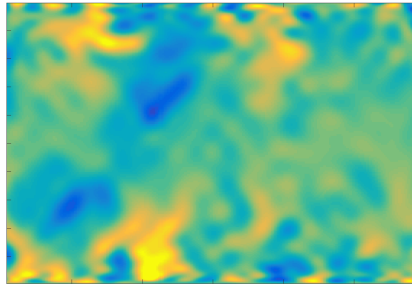
- ▶ **Large scales** carry most of kinetic energy, responsible for flow dynamics and transportation of matter
- ▶ **Small scales** are more related to dissipation properties; more universal



Sample streamwise velocity field of a channel flow ( $Re_\tau = 550$ ) and a synthesized spectrum (all scales)

# Turbulence is multiscale

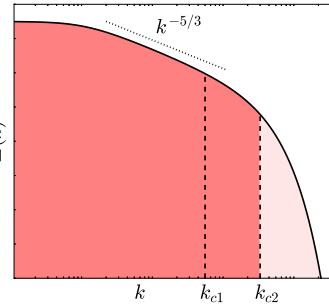
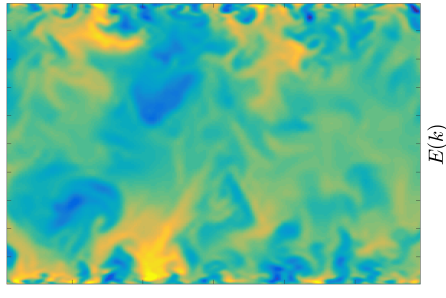
- ▶ **Large scales** carry most of kinetic energy, responsible for flow dynamics and transportation of matter
- ▶ **Small scales** are more related to dissipation properties; more universal



Sample streamwise velocity field of a channel flow ( $Re_\tau = 550$ ) and a synthesized spectrum (large scales)

# Turbulence is multiscale

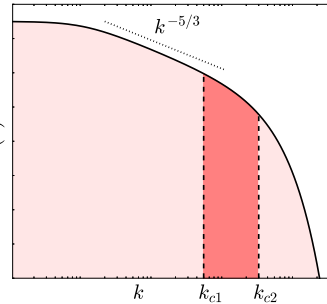
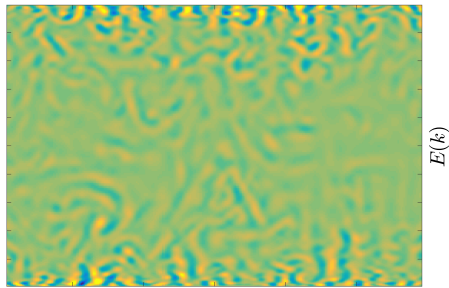
- ▶ **Large scales** carry most of kinetic energy, responsible for flow dynamics and transportation of matter
- ▶ **Small scales** are more related to dissipation properties; more universal



Sample streamwise velocity field of a channel flow ( $Re_\tau = 550$ ) and a synthesized spectrum (large scales)

# Turbulence is multiscale

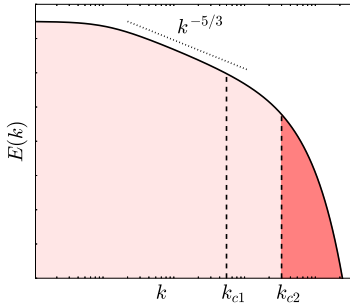
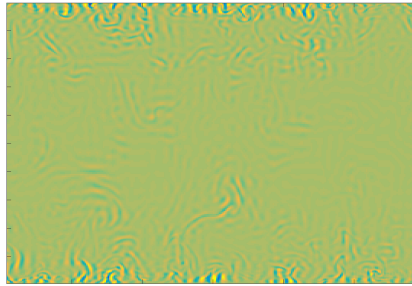
- ▶ **Large scales** carry most of kinetic energy, responsible for flow dynamics and transportation of matter
- ▶ **Small scales** are more related to dissipation properties; more universal



Sample streamwise velocity field of a channel flow ( $Re_\tau = 550$ ) and a synthesized spectrum (mid scales)

# Turbulence is multiscale

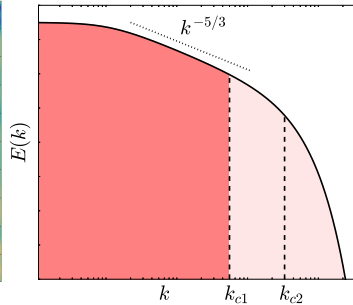
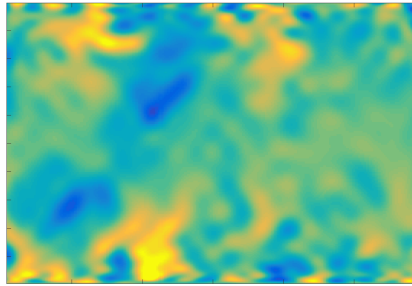
- ▶ **Large scales** carry most of kinetic energy, responsible for flow dynamics and transportation of matter
- ▶ **Small scales** are more related to dissipation properties; more universal



Sample streamwise velocity field of a channel flow ( $Re_\tau = 550$ ) and a synthesized spectrum (small scales)

# Turbulence is multiscale

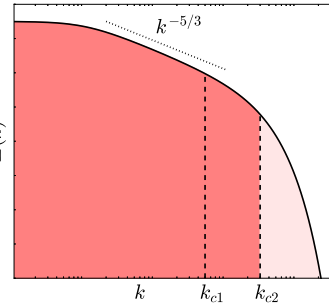
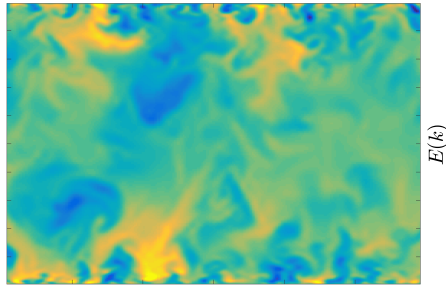
- ▶ **Large scales** carry most of kinetic energy, responsible for flow dynamics and transportation of matter
- ▶ **Small scales** are more related to dissipation properties; more universal



Sample streamwise velocity field of a channel flow ( $Re_\tau = 550$ ) and a synthesized spectrum (large scales)

# Turbulence is multiscale

- ▶ **Large scales** carry most of kinetic energy, responsible for flow dynamics and transportation of matter
- ▶ **Small scales** are more related to dissipation properties; more universal



Sample streamwise velocity field of a channel flow ( $Re_\tau = 550$ ) and a synthesized spectrum (large scales)

# Importance of small scales

- ▶ Better insight on turbulence physics (dissipation, coherent structures)
- ▶ Validation of turbulence models (Large Eddy Simulation)

# Importance of small scales

- ▶ Better insight on turbulence physics (dissipation, coherent structures)
- ▶ Validation of turbulence models (Large Eddy Simulation)



Turbulent boundary layers (photo credit: Juan A. Sillero)

# Importance of small scales

- ▶ Better insight on turbulence physics (dissipation, coherent structures)
- ▶ Validation of turbulence models (Large Eddy Simulation)



Turbulent combustion and reacting flows (photo credit: TESLa, Colorado University)

# Motivations of the thesis

**Problem:** cannot access a full range of scales

- ▶ **Experiments:**
  - ▶ **Optical measurement** (PIV, PTV): compromise between frequency, resolution and field-of-view
  - ▶ **Hot wire anemometer** (HWA): high frequency but point-measurement
- ▶ **Simulations:** only accessible from Direct Numerical Simulation, but
  - ▶ limited to low to moderate  $Re$  and/or simple geometries
  - ▶ excessive computational cost to converge statistics

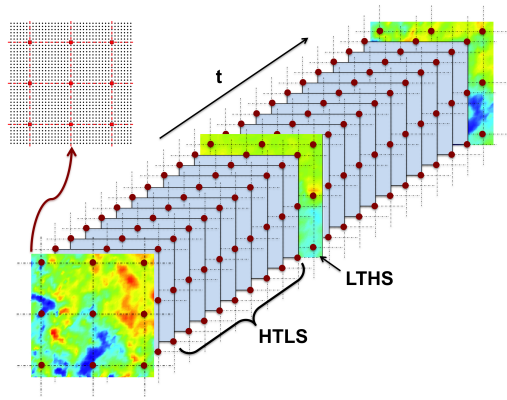
**Our main objectives:**

- ▶ Computational methods to reconstruct partly unresolved scales
- ▶ Model assessment using numerical database

# Numerical experiment setup

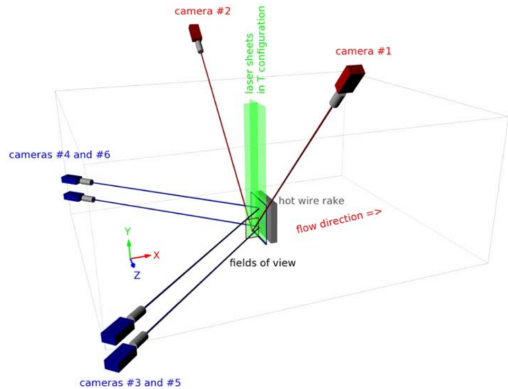
## Setup of complementary measurements:

- ▶ High-Time-Low-Space (**HTLS**) of size  $Q \times N$
- ▶ Low-Time-High-Space (**LTHS**) of size  $P \times M$  ( $Q \ll P, M \ll N$ )

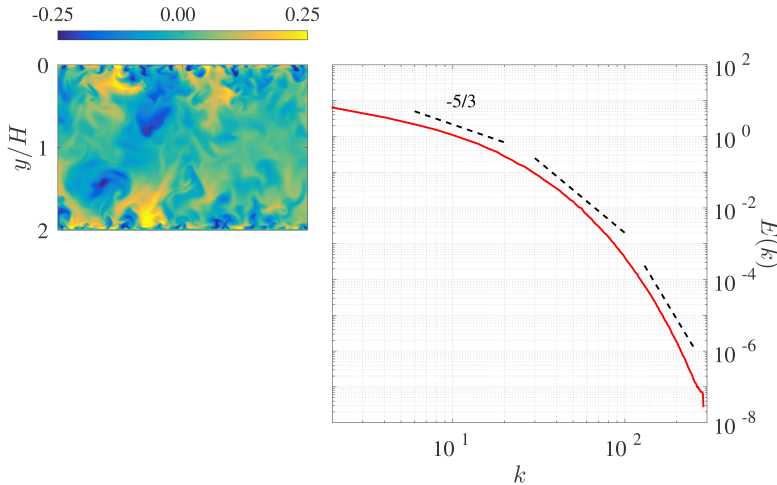


## Example: WALLTURB project [Coudert et al., 2011]

- ▶ Complementary measurements: **HWA** as **HTLS** ( $11 \times 13$ , 30 kHz), **PIV** as **LTHS** ( $143 \times 161$ , 4 Hz)
- ▶ Reconstruct **HTHS** ( $143 \times 161$ , 30 kHz) using regression  
[Dekou et al., 2016]

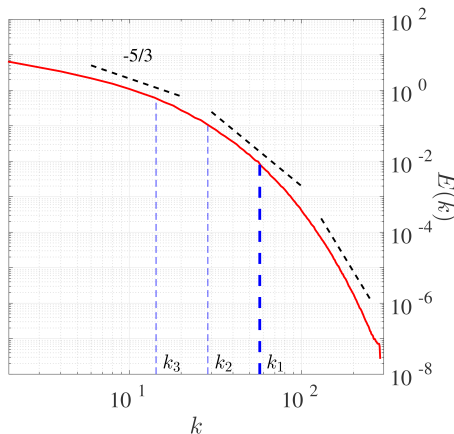
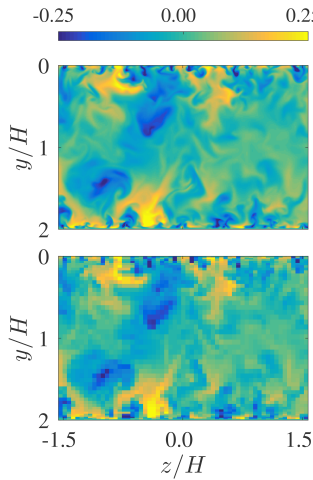


# Problem definition: inverse problem



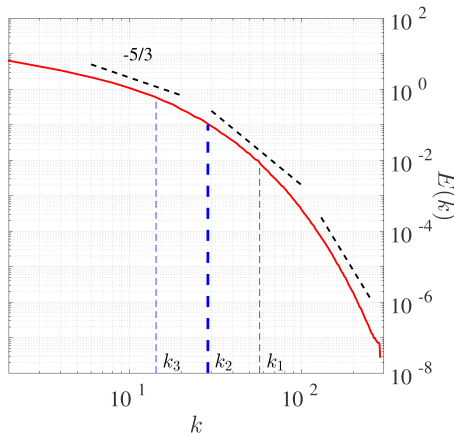
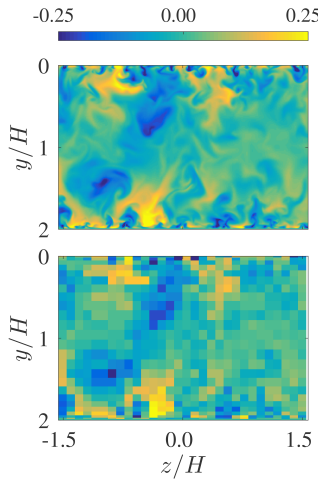
A sample streamwise velocity field from DNS of a turbulent channel flow ( $Re_\tau = 550$ ) and the spectrum in space

# Problem definition: inverse problem



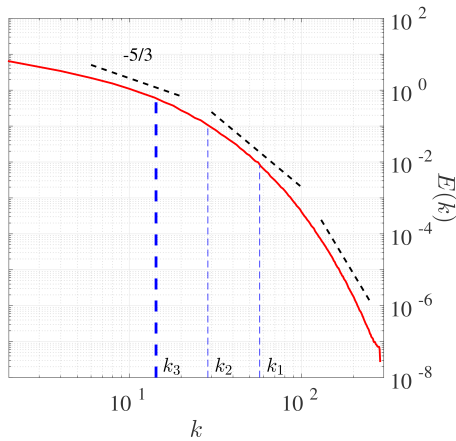
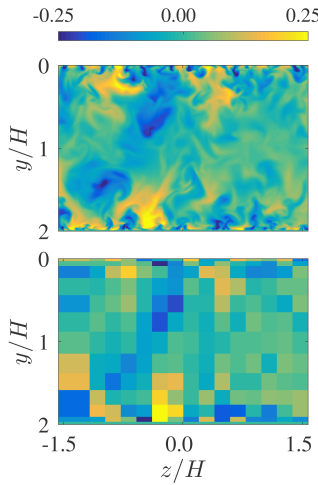
Subsample by  $5 \times 5$  ( $k_1$ )

# Problem definition: inverse problem



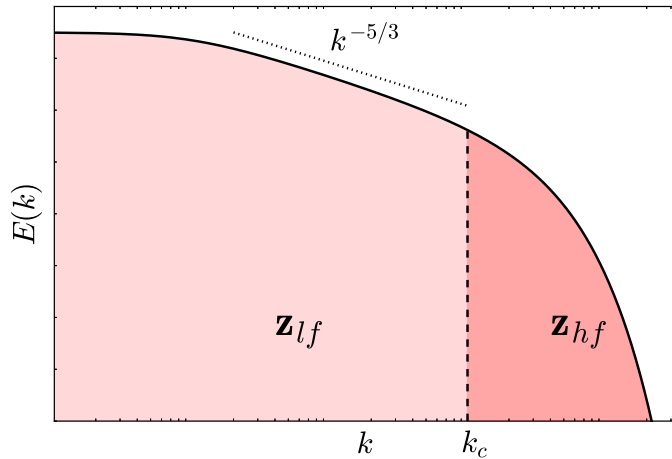
Subsample by  $10 \times 10$  ( $k_2$ )

# Problem definition: inverse problem

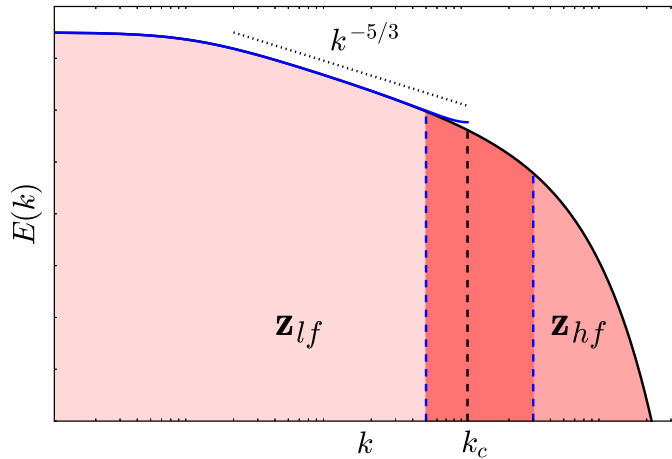


Subsample by  $20 \times 20$  ( $k_3$ )

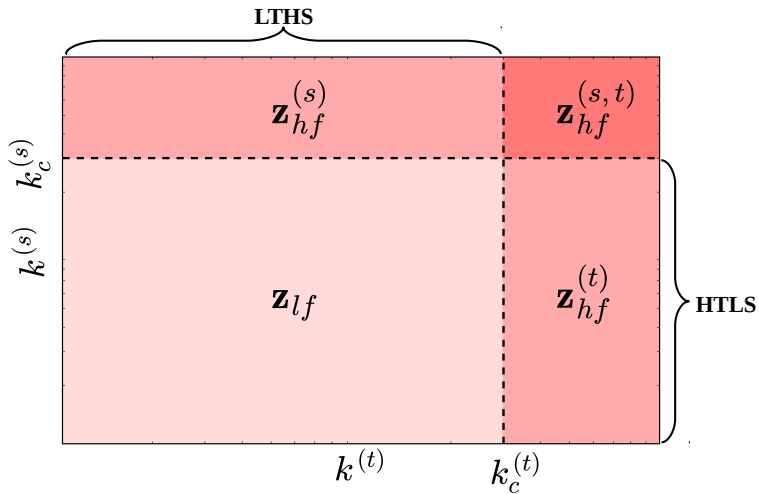
# Problem 1: mapping functions between small & large scales



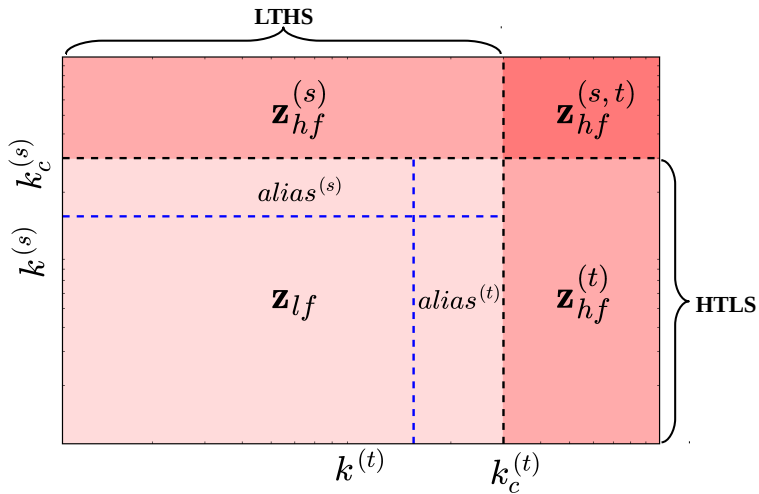
# Problem 1: mapping functions between small & large scales



## Problem 2: fusion of complementary measurements



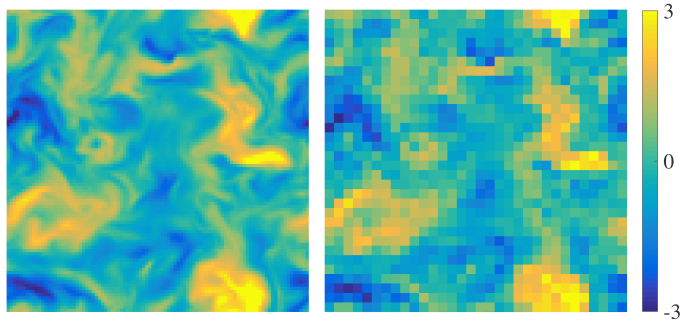
# Problem 2: fusion of complementary measurements



# Numerical datasets

Two numerical datasets of full resolution are used:

- (i.) **Isotropic turbulence**: 37 blocks of 3D field of  $96^3$  ( $Re_\lambda = 90, 384^3$ )
- (ii.) **Turbulent channel flow**: 10000 snapshots of  $257 \times 288$ ,  $Re_\tau = 550$

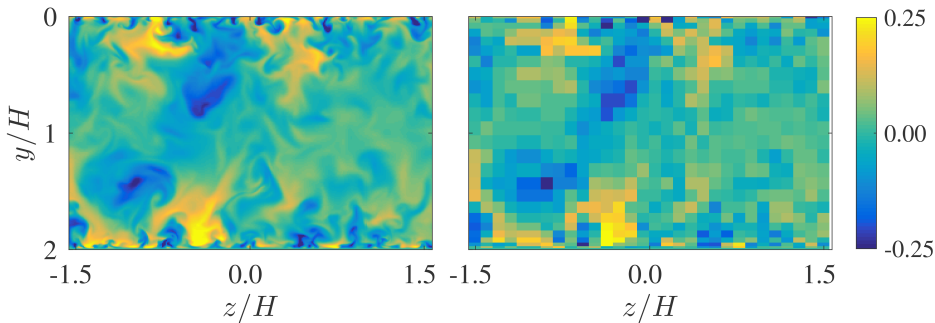


Sample streamwise velocity field of isotropic turbulence at  $Re_\lambda = 90$

# Numerical datasets

Two numerical datasets of full resolution are used:

- (i.) **Isotropic turbulence**: 37 blocks of 3D field of  $96^3$  ( $Re_\lambda = 90, 384^3$ )
- (ii.) **Turbulent channel flow**: 10000 snapshots of  $257 \times 288$ ,  $Re_\tau = 550$



Sample streamwise velocity field of the channel flow at  $Re_\tau = 550$

# Approaches in the literature

## Reconstruction methods in turbulence studies:

- ▶ **Least-square** regression [Durgesh and Naughton, 2010]
- ▶ **POD** reduced-order model [Bonnet et al., 1994]
- ▶ **Data assimilation** using Kalman filter [Papadakis et al., 2010, Tu et al., 2013]
- ▶ **Physical priors**: div-curl regularization [Corpetti et al., 2002],  
vortex-in-cell [Schneiders et al., 2014]

# Approaches in the literature

## Reconstruction methods in turbulence studies:

- ▶ **Least-square** regression [Durgesh and Naughton, 2010]
- ▶ **POD** reduced-order model [Bonnet et al., 1994]
- ▶ **Data assimilation** using Kalman filter [Papadakis et al., 2010, Tu et al., 2013]
- ▶ **Physical priors**: div-curl regularization [Corpetti et al., 2002],  
vortex-in-cell [Schneiders et al., 2014]



# Approaches in the present work

## Approach 1: learn a mapping function between scales

**Objective:**  $\mathbf{z}_\ell \in \mathbb{R}^Q \mapsto \mathbf{z}_h \in \mathbb{R}^P, P \gg Q$

- ▶ **Regression:** as set of coefficients
- ▶ **Coupled dictionary learning:** coupled representations of LR/HR

## Approach 2: fusion of complementary measurements

**Objective:** find  $\mathbf{z}$  given two measurements  $\mathbf{x}$  and  $\mathbf{y}$

- ▶ **Non-local means:** self similarity of flow structures
- ▶ **Bayesian fusion:** *maximum a posteriori* estimate  $p(\mathbf{z} | \mathbf{x}, \mathbf{y})$

# Regression

Learn  $f$  from training samples  $(\mathbf{y}_t, \mathbf{z}_t)$ :

$$f : \mathbf{y}_t \mapsto \hat{\mathbf{z}}_t = f(\mathbf{y}_t) + \mathbf{n}^{(t)} \approx \mathbf{B}^\top \mathbf{y}_t$$

- ▶ Linear regression:

$$\mathbf{B} = \underset{\mathbf{B}}{\operatorname{argmin}} \left\{ \underbrace{\|\mathbf{Y}\mathbf{B} - \mathbf{Z}\|_2^2}_{\text{data misfit}} + \underbrace{\lambda g(\mathbf{B})}_{\text{penalty}} \right\}$$

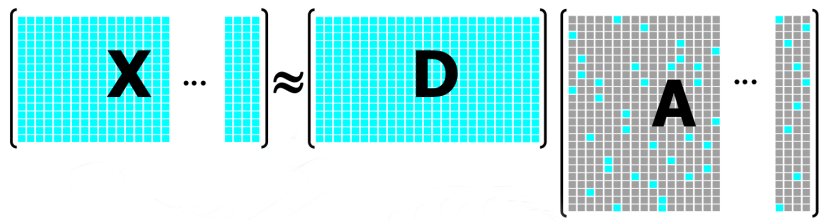
- ▶ **Ridge regression**:  $g(\mathbf{B}) = \|\mathbf{B}\|_2^2$
- ▶ **LASSO**:  $g(\mathbf{B}) = \|\mathbf{B}\|_1$
- ▶ Nonlinear regression: projection into kernel space (**KRR**)
- ▶ Parameter estimation: *bias-variance* trade-off, *k-fold* cross validation

# Dictionary learning: a generalization of POD

- ▶ Data representation: linear transformation via a “*dictionary*”

$$\mathbf{X} = \mathbf{D}\mathbf{A}$$

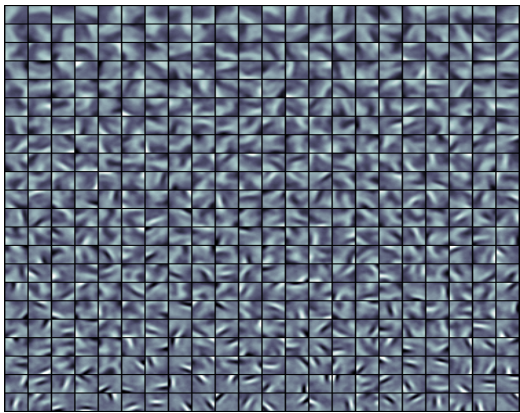
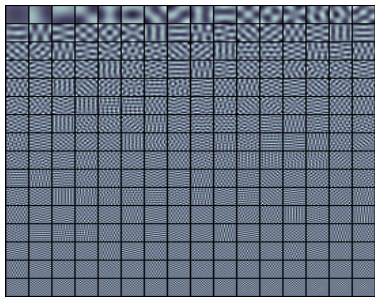
- ▶ Dictionary learning:  $\mathbf{D}$  is *redundant* (or *overcomplete*),  $\mathbf{A}$  is *sparse*



- ▶ Dictionary learning as an alternating optimization problem:

$$(\mathbf{D}, \mathbf{A}) = \operatorname{argmin}_{\mathbf{D}, \mathbf{A}} \left\{ \|\mathbf{X} - \mathbf{D}\mathbf{A}\|_2^2 + \lambda \|\mathbf{A}\|_1 \right\}$$

# Orthogonal vs redundant bases

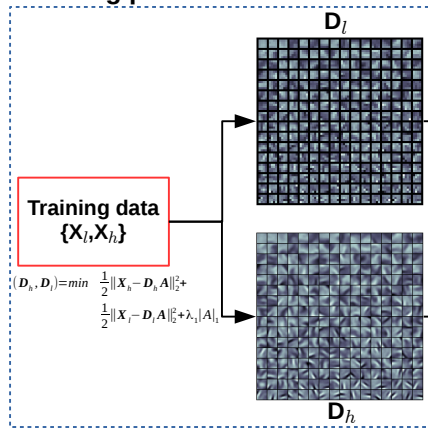


Dictionaries learned by POD and DL from the set of HR patches of size  $16 \times 16$

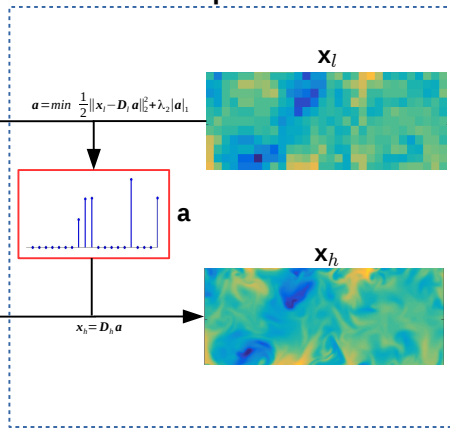
# Reconstruct HR fields using coupled dictionary learning

- Motivated by single image super-resolution [Yang et al., 2010]
- Two steps: *learning* (offline) and *reconstruction* (online)

## Learning phase



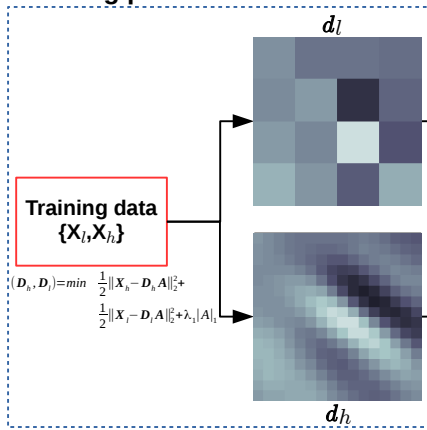
## Reconstruction phase



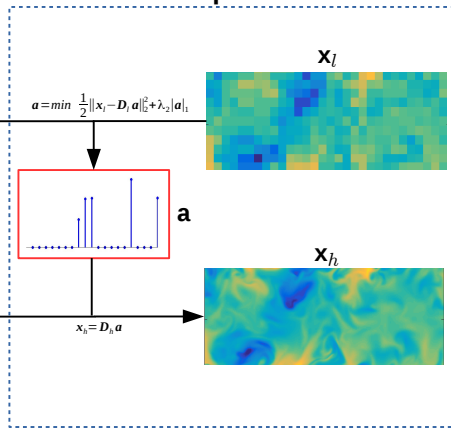
# Reconstruct HR fields using coupled dictionary learning

- Motivated by single image super-resolution [Yang et al., 2010]
- Two steps: *learning* (offline) and *reconstruction* (online)

## Learning phase



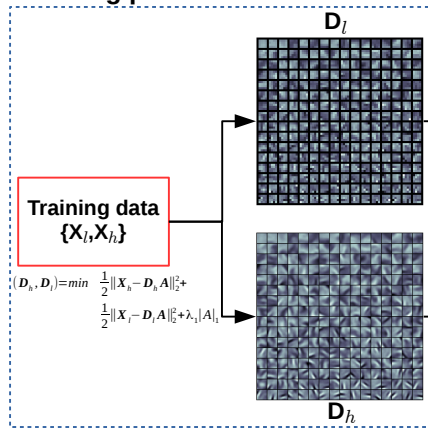
## Reconstruction phase



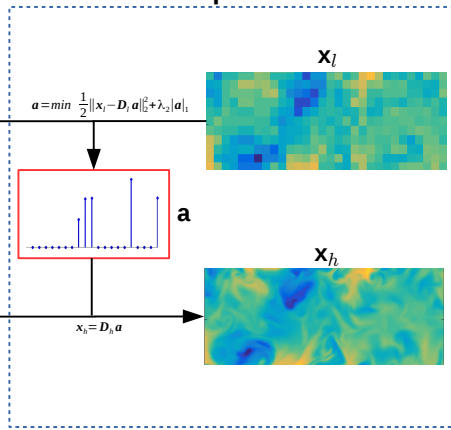
# Reconstruct HR fields using coupled dictionary learning

- Motivated by single image super-resolution [Yang et al., 2010]
- Two steps: *learning* (offline) and *reconstruction* (online)

## Learning phase



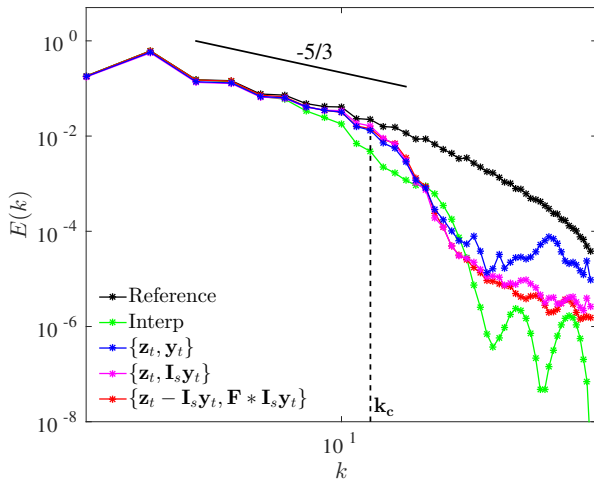
## Reconstruction phase



# Numerical experiment setup for coupled dictionary learning

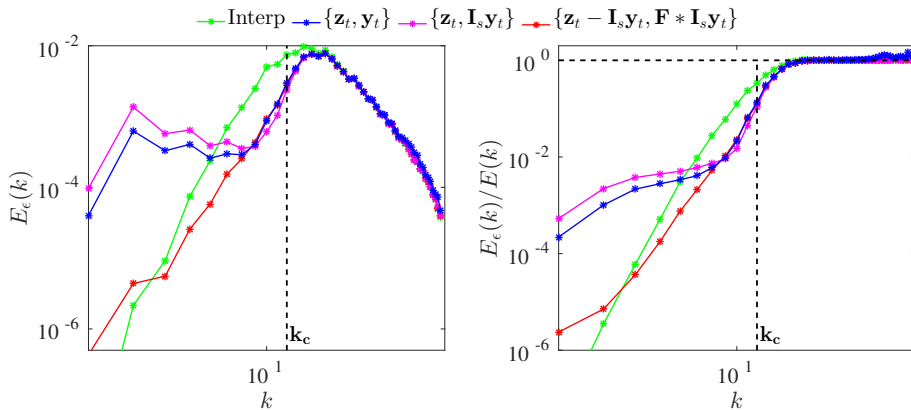
- ▶ **Subsampling:**  $y_t \triangleq \mathbb{S}_s z_t$
- ▶ **Downsampling case:**  $y_t \triangleq \mathbb{S}_s \mathbb{L}_s z_t$
- ▶ **Patch-based approach:** localized information
- ▶ **Parameters:** patch size, number of patches, sparsity constraints (for the learning and reconstruction step)
- ▶ **Preprocessing methods** by coupling:
  - ▶ High and low resolution,  $\{z_t, y_t\}$
  - ▶ Reference and interpolated high resolution,  $\{z_t, \mathbb{I}_s y_t\}$
  - ▶ Residual and features (derivatives),  $\{z_t - \mathbb{I}_s y_t, \mathbb{F} * \mathbb{I}_s y_t\}$

## Results: energy spectra



Energy spectra (2D) of reference, interpolation and reconstruction by 3 coupled dictionary learning approaches (sampling ratio of  $4 \times 4$ )

# Results: spectra of the error



2D error spectra (with and without normalization) of interpolation and reconstruction by 3 coupled dictionary learning approaches (sampling ratio of  $4 \times 4$ )

# A generalization of non-local means

**Objective:** propagating small scales from LTHS planes based on the similarity levels between large scales

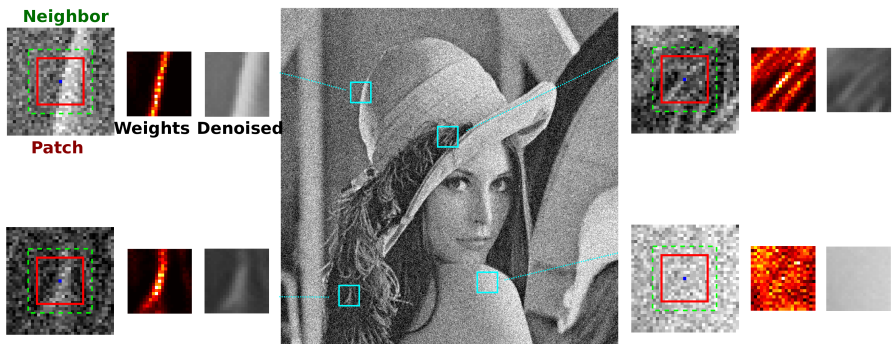


Figure: Non-local means for denoising [Buades et al., 2005]

# A generalization of non-local means

**Objective:** propagating small scales from LTHS planes based on the similarity levels between large scales

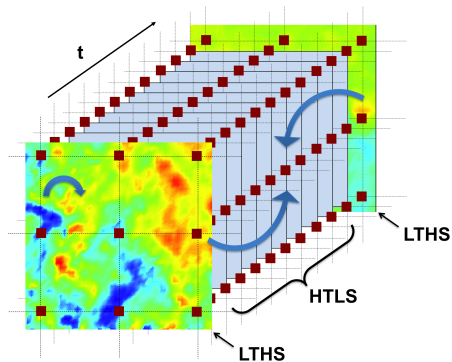


Figure: Propagation of small scales, inspired by video super-resolution [Protter et al., 2009]

# The principle: weighted average using non-local similarity

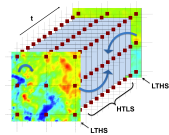
- ▶ **Principle:** video super-resolution [Protter et al., 2009]

$$\hat{\mathbf{z}}_{t_o}[k] = \frac{\sum_{t \in \mathcal{N}_{t_o}} \sum_{i \in \mathcal{N}_k} w[k, i, t] \mathbf{y}_t[i]}{\sum_{t \in \mathcal{N}_{t_o}} \sum_{i \in \mathcal{N}_k} w[k, i, t]}$$

where  $w[k, i, t] = \exp\left(-\frac{1}{2\sigma^2} \|\mathcal{R}_s^k \mathbf{y}_{t_o} - \mathcal{R}_s^i \mathbf{y}_t\|_2^2\right)$

- ▶ **Modification:** reconstruct small scales  $\mathbf{b}_{t_o} = \mathbf{x}_{t_o} - \mathbb{I}_s \mathbb{S}_s \mathbf{x}_{t_o}$  only

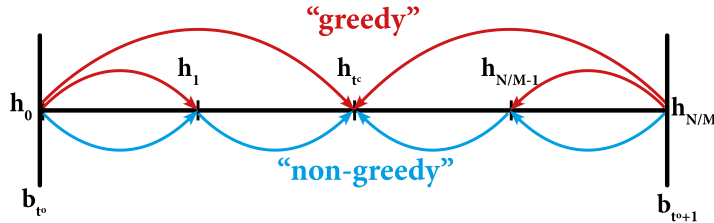
$$\hat{\mathbf{b}}_t[k] = \frac{\sum_{i \in \mathcal{N}_k} w_0[k, i, t] \mathbf{b}_{t_o}[i] + \sum_{i \in \mathcal{N}_k} w_1[k, i, t] \mathbf{b}_{t_o+1}[i]}{\sum_{i \in \mathcal{N}_k} w_0[k, i, t] + \sum_{i \in \mathcal{N}_k} w_1[k, i, t]}$$



# Non-local means: schemes and parameters

## ► Parameters:

- ▶ Filter parameter:  $\sigma$
- ▶ Neighbor sizes  $\#(N_k)$
- ▶ Patch size:  $\#\left(\mathcal{R}_s^k y_t\right)$
- ▶ Greedy and non-greedy propagation schemes



# Bayesian fusion: the framework

- ▶ Motivation: fusion of multi- and hyper-spectral images [Hardie et al., 2004]
- ▶ Bayesian fusion: *maximum a posteriori*

$$\hat{\mathbf{z}} = \operatorname{argmax}_{\mathbf{z}} \{ p(\mathbf{z} | \mathbf{x}, \mathbf{y}) \}$$

- ▶ Applying *Bayes' theorem*:

$$p(\mathbf{z} | \mathbf{x}, \mathbf{y}) = \frac{p(\mathbf{x}, \mathbf{y} | \mathbf{z}) p(\mathbf{z})}{p(\mathbf{x}, \mathbf{y})} = \frac{p(\mathbf{x} | \mathbf{z}) p(\mathbf{y} | \mathbf{z}) p(\mathbf{z})}{p(\mathbf{x}, \mathbf{y})}$$

- ▶ *Non-informative (improper) prior*, i.e.  $p(\mathbf{z})$  is constant,:  
$$\hat{\mathbf{z}} = \operatorname{argmax}_{\mathbf{z}} \{ p(\mathbf{z} | \mathbf{x}) p(\mathbf{z} | \mathbf{y}) \}$$

# Single models and closed-form fusion formula

- ▶ Single models:

$$\mathbf{z} = \mathbb{I}_t \mathbf{x} + \mathbf{h}_t \quad (\mathbb{I}_t \mathbf{x} \perp\!\!\!\perp \mathbf{h}_t)$$

$$\mathbf{z} = \mathbb{I}_s \mathbf{y} + \mathbf{h}_s \quad (\mathbb{I}_s \mathbf{y} \perp\!\!\!\perp \mathbf{h}_s)$$

- ▶ Multivariate Gaussian probability:

$$p(\mathbf{z} | \mathbf{x}) = \frac{1}{(2\pi)^{PN/2} |\Sigma_{\mathbf{h}_t}|^{1/2}} \exp \left\{ -\frac{1}{2} (\mathbf{z} - \mathbb{I}_t \mathbf{x})^\top \Sigma_{\mathbf{h}_t}^{-1} (\mathbf{z} - \mathbb{I}_t \mathbf{x}) \right\}$$

( $\Sigma_{\mathbf{h}_t} = \mathbf{h}_t \mathbf{h}_t^\top$ : covariance matrix)

- ▶ Closed-form solution:

$$\hat{\mathbf{z}} = \left( \Sigma_{\mathbf{h}_s}^{-1} + \Sigma_{\mathbf{h}_t}^{-1} \right)^{-1} \left( \Sigma_{\mathbf{h}_s}^{-1} \mathbb{I}_s \mathbf{y} + \Sigma_{\mathbf{h}_t}^{-1} \mathbb{I}_t \mathbf{x} \right)$$

# Simplification and interpretation of the fusion formula

**Simplification:**  $\Sigma_{h_s}$  and  $\Sigma_{h_t}$  are diagonal

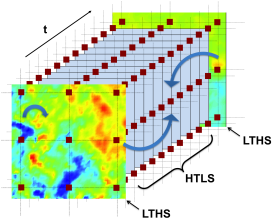
$$\hat{\mathbf{z}}[i, t] = \frac{\sigma_{h_s}^2[i, t]}{\sigma_{h_s}^2[i, t] + \sigma_{h_t}^2[i, t]} \mathbb{I}_t \mathbf{x}[i, t] + \frac{\sigma_{h_t}^2[i, t]}{\sigma_{h_s}^2[i, t] + \sigma_{h_t}^2[i, t]} \mathbb{I}_s \mathbf{y}[i, t]$$

# Simplification and interpretation of the fusion formula

**Simplification:**  $\Sigma_{h_s}$  and  $\Sigma_{h_t}$  are diagonal

$$\hat{\mathbf{z}}[i, t] = \frac{\sigma_{h_s}^2[i, t]}{\sigma_{h_s}^2[i, t] + \sigma_{h_t}^2[i, t]} \mathbb{I}_t \mathbf{x}[i, t] + \frac{\sigma_{h_t}^2[i, t]}{\sigma_{h_s}^2[i, t] + \sigma_{h_t}^2[i, t]} \mathbb{I}_s \mathbf{y}[i, t]$$

**Interpretation:**  $\hat{\mathbf{z}}$  is fused from 2 data sources  $\mathbb{I}_t \mathbf{x}$  and  $\mathbb{I}_s \mathbf{y}$  via weighted coefficients  $\sigma_{h_s}^2$  and  $\sigma_{h_t}^2$  (learned from  $\mathbf{x}$  and  $\mathbf{y}$  only).

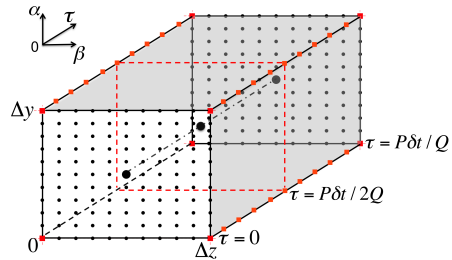


# Models performances: loss of energy and NRMSE

$\mathbf{z}^*$ ,  $\hat{\mathbf{z}}$  and  $\mathbb{L}\mathbf{z}$  are reference, reconstructed and filtered fields

- ▶ Loss of energy:

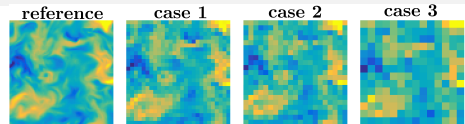
$$\Delta\kappa = \frac{\sum_{j \in \mathbb{J}} \mathbf{z}_j^2 - \sum_{j \in \mathbb{J}} [\mathbb{L}\mathbf{z}]_j^2}{\sum_{j \in \mathbb{J}} \mathbf{z}_j^2}$$



- ▶ Normalized Root Mean Squared Error (NRMSE):

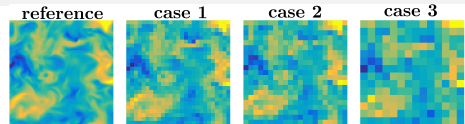
$$\epsilon = \left( \frac{\sum_t \sum_{j \in \mathbb{J}} (\hat{\mathbf{z}}_{t,j} - \mathbf{z}_{t,j})^2}{\sum_t \sum_{j \in \mathbb{J}} \mathbf{z}_{t,j}^2} \right)^{1/2}$$

# NRMSEs on isotropic turbulence data



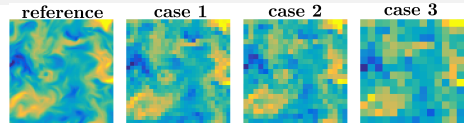
Method	$(\frac{P}{Q}, \frac{N}{M})$ $\Delta\kappa$	$\bar{\epsilon}$			$\epsilon_{max}$		
		Case 1	Case 2	Case 3	Case 1	Case 2	Case 3
		$(3^2, 4)$ 1%	$(4^2, 6)$ 3%	$(6^2, 8)$ 7%	$(3^2, 4)$ 1%	$(4^2, 6)$ 3%	$(6^2, 8)$ 7%
$\mathbb{I}_s \mathbf{y}$		0.19	0.28	0.43	0.22	0.35	0.52
$\mathbb{I}_t \mathbf{x}$		0.13	0.23	0.31	0.19	0.28	0.42
RR		0.14	0.23	0.35	0.20	0.34	0.50
KRR		0.13	0.23	0.34	0.20	0.34	0.49
Greedy propag		0.11	0.20	0.32	0.18	0.33	0.51
Non-greedy propag		0.11	0.19	0.30	0.17	0.31	0.46
Fusion (LG)		0.11	0.18	0.27	0.17	0.26	0.41
Fusion (BF)		0.11	0.18	0.26	0.17	0.26	0.40

# NRMSEs on isotropic turbulence data



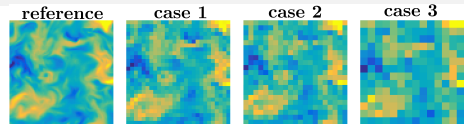
Method	$(\frac{P}{Q}, \frac{N}{M})$ $\Delta\kappa$	$\bar{\epsilon}$			$\epsilon_{max}$		
		Case 1	Case 2	Case 3	Case 1	Case 2	Case 3
		$(3^2, 4)$ 1%	$(4^2, 6)$ 3%	$(6^2, 8)$ 7%	$(3^2, 4)$ 1%	$(4^2, 6)$ 3%	$(6^2, 8)$ 7%
$\mathbb{I}_s \mathbf{y}$		0.19	0.28	0.43	0.22	0.35	0.52
$\mathbb{I}_t \mathbf{x}$		0.13	0.23	0.31	0.19	0.28	0.42
RR		0.14	0.23	0.35	0.20	0.34	0.50
KRR		0.13	0.23	0.34	0.20	0.34	0.49
Greedy propag		0.11	0.20	0.32	0.18	0.33	0.51
Non-greedy propag		0.11	0.19	0.30	0.17	0.31	0.46
Fusion (LG)		0.11	0.18	0.27	0.17	0.26	0.41
Fusion (BF)		0.11	0.18	0.26	0.17	0.26	0.40

# NRMSEs on isotropic turbulence data



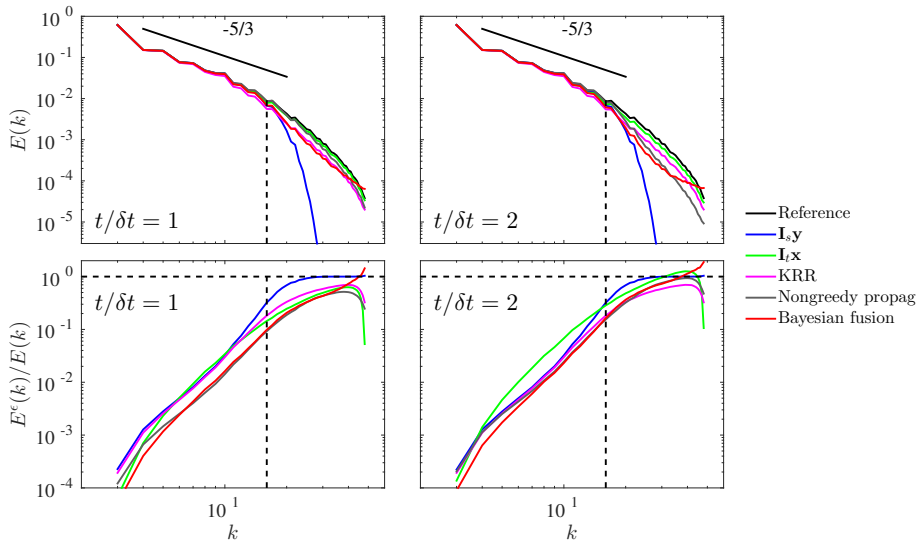
Method	$(\frac{P}{Q}, \frac{N}{M})$ $\Delta\kappa$	$\bar{\epsilon}$			$\epsilon_{max}$		
		Case 1	Case 2	Case 3	Case 1	Case 2	Case 3
		$(3^2, 4)$ 1%	$(4^2, 6)$ 3%	$(6^2, 8)$ 7%	$(3^2, 4)$ 1%	$(4^2, 6)$ 3%	$(6^2, 8)$ 7%
$\mathbb{I}_s \mathbf{y}$		0.19	0.28	0.43	0.22	0.35	0.52
$\mathbb{I}_t \mathbf{x}$		0.13	0.23	0.31	0.19	0.28	0.42
RR		0.14	0.23	0.35	0.20	0.34	0.50
KRR		0.13	0.23	0.34	0.20	0.34	0.49
Greedy propag		0.11	0.20	0.32	0.18	0.33	0.51
Non-greedy propag		0.11	0.19	0.30	0.17	0.31	0.46
Fusion (LG)		0.11	0.18	0.27	0.17	0.26	0.41
Fusion (BF)		0.11	0.18	0.26	0.17	0.26	0.40

# NRMSEs on isotropic turbulence data

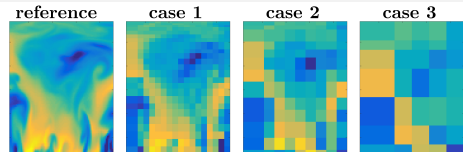


Method	$(\frac{P}{Q}, \frac{N}{M})$ $\Delta\kappa$	$\bar{\epsilon}$			$\epsilon_{max}$		
		Case 1	Case 2	Case 3	Case 1	Case 2	Case 3
		$(3^2, 4)$ 1%	$(4^2, 6)$ 3%	$(6^2, 8)$ 7%	$(3^2, 4)$ 1%	$(4^2, 6)$ 3%	$(6^2, 8)$ 7%
$\mathbb{I}_s \mathbf{y}$		0.19	0.28	0.43	0.22	0.35	0.52
$\mathbb{I}_t \mathbf{x}$		0.13	0.23	0.31	0.19	0.28	0.42
RR		0.14	0.23	0.35	0.20	0.34	0.50
KRR		0.13	0.23	0.34	0.20	0.34	0.49
Greedy propag		<b>0.11</b>	0.20	0.32	0.18	0.33	0.51
Non-greedy propag		<b>0.11</b>	0.19	0.30	<b>0.17</b>	0.31	0.46
Fusion (LG)		<b>0.11</b>	<b>0.18</b>	0.27	<b>0.17</b>	<b>0.26</b>	0.41
Fusion (BF)		<b>0.11</b>	<b>0.18</b>	<b>0.26</b>	<b>0.17</b>	<b>0.26</b>	<b>0.40</b>

# Spectra of reconstructed fields by various methods



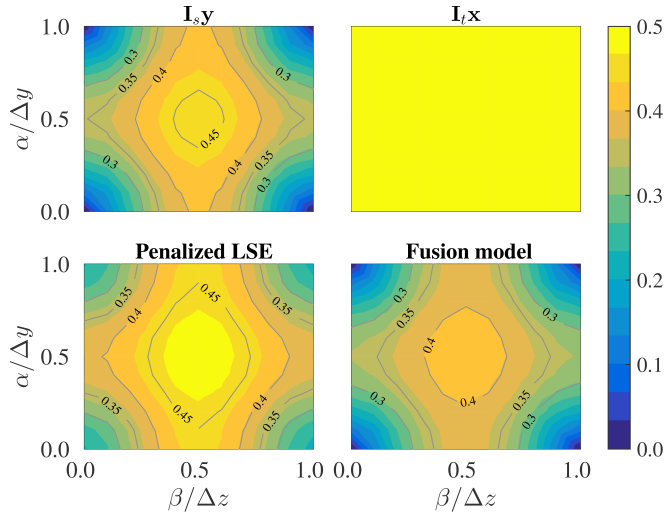
# NRMSEs on turbulent channel flow data



Method	$\bar{\epsilon}$			$\epsilon_{max}$		
	Case 1	Case 2	Case 3	Case 1	Case 2	Case 3
	$(\frac{P}{Q}, \frac{N}{M})$	$(5^2, 4)$	$(10^2, 10)$	$(20^2, 20)$	$(5^2, 4)$	$(10^2, 10)$
$\mathbb{I}_s \mathbf{y}$	0.14	0.36	0.68	0.16	0.47	0.85
$\mathbb{I}_t \mathbf{x}$	0.11	0.32	0.54	0.18	0.55	0.85
RR	0.12	0.34	0.64	0.15	0.49	0.78
Fusion (BF)	<b>0.08</b>	<b>0.25</b>	<b>0.46</b>	<b>0.13</b>	<b>0.43</b>	<b>0.73</b>

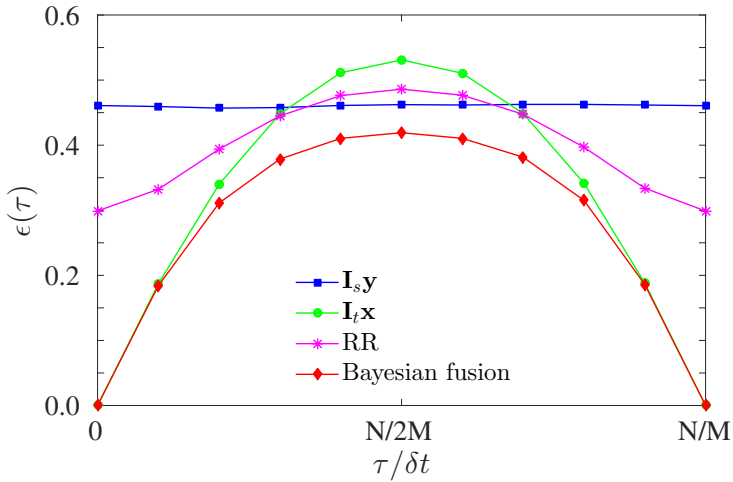
\*Errors are estimated in the middle of the channel,  $y/H = [0.5, 1.5]$

# NRMSEs as functions of position in space



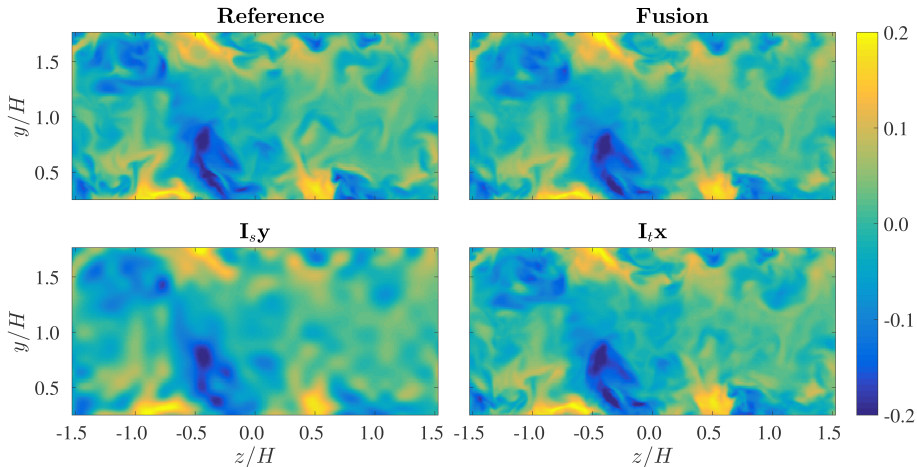
NRMSEs averaged over all points at  $y/H = [0.5, 1.5]$  and  $(\alpha, \beta) = (\Delta\alpha/2, \Delta\beta/2)$

# NRMSEs as functions of position in time



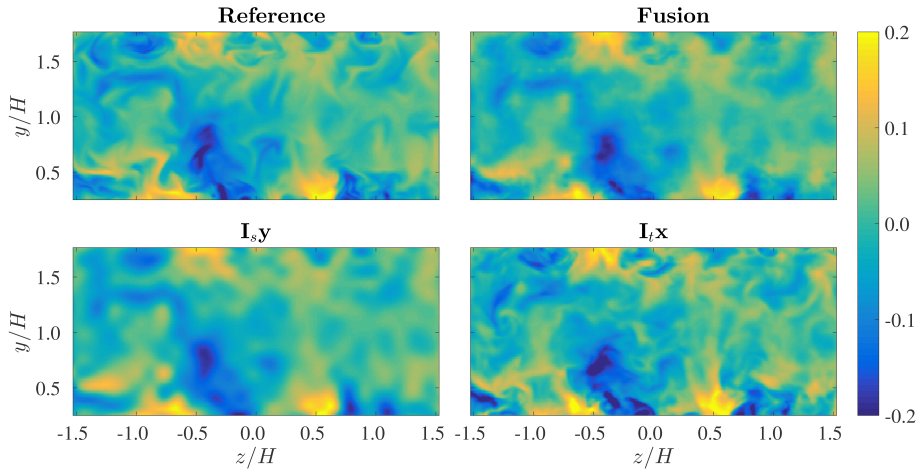
NRMSEs averaged over all blocks bounded by 4 HTLS measurements at  $y/H = [0.5, 1.5]$  and  $\tau = N/2M$

# A sample velocity field



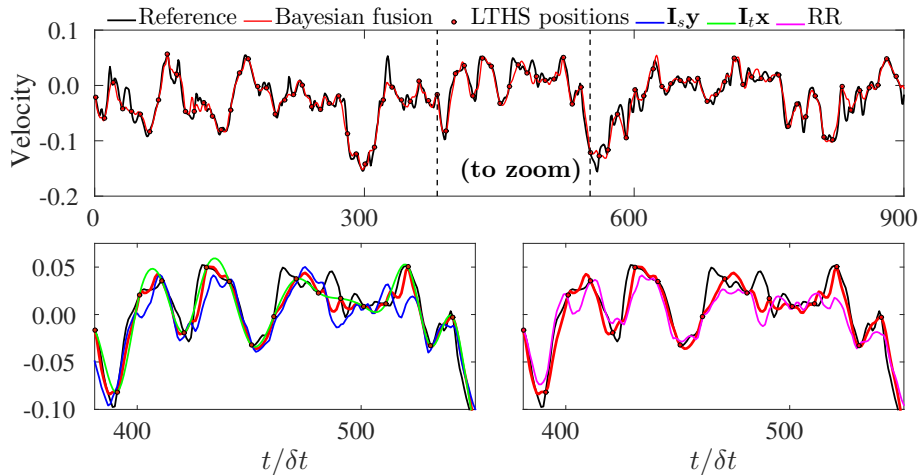
A snapshot of reconstructed and reference streamwise velocity field at  $\tau = 2$

# A sample velocity field



A snapshot of reconstructed and reference streamwise velocity field at  $\tau = N/2M = 6$

# A sample time evolution



A time evolution of reconstructed and reference streamwise velocity at the center of the channel,  
 $y/H = 1$  and  $(\alpha, \beta) = (\Delta\alpha/2, \Delta\beta/2)$

# Conclusions

- ▶ Adaptive single models over-perform single interpolation methods
- ▶ Benefits are observed by combining complementary information
- ▶ Problems of sampling and aliasing should be considered in future sensing systems
- ▶ Problems in turbulence are essentially different from image processing
- ▶ Turbulence is hard, but complex learning algorithms are promising
- ▶ Learning is powerful, but physics is also crucial

# Suggestions for future works

## (i) On the models

- ▶ Using physical prior: Navier-Stokes, divergence-free, turbulence spectra
- ▶ Highly nonlinear mapping functions with deep neural network, potentially combined with sparse prior
- ▶ Ensemble of models: further exploit the advantages of all models
- ▶ Combine fusion and dictionary learning: ADMM

$$\mathbf{z} = \mathbf{D}\mathbf{A}s.t.\{\mathbf{D}, \mathbf{A}\} = \operatorname{argmin}_{\mathbf{D}, \mathbf{A}} \left\{ \frac{1}{2} \|\mathbf{S}_t \mathbf{D}\mathbf{A} - \mathbf{x}\|_{\Sigma_{h_t}}^2 + \frac{1}{2} \|\mathbf{S}_s \mathbf{D}\mathbf{A} - \mathbf{y}\|_{\Sigma_{h_s}}^2 + \lambda \|\mathbf{A}\|_1 \right\}$$

# Suggestions for future works

## (ii) Co-conception design

- ▶ Reconstruction of three-component velocity fields and cross-component quantities (cross-correlation, vorticity)
- ▶ Handle aliasing
- ▶ Increase the resolution of PIV measurements by different setups
- ▶ Design new challenging measurements

# Main contributions

This work has resulted in:

Nguyen et al., (2015). “A Bayesian fusion model for space-time reconstruction of finely resolved velocities in turbulent flows from low resolution measurements”. In: *Journal of Statistical Mechanics: Theory and Experiment* 2015.10, P10008.

and has presented at:

- ▶ 15th European Turbulence conference, Delft, Netherlands
- ▶ GDR Turbulence, Grenoble, France

Codes are available at:

<https://github.com/linhvannguyen/>

The screenshot shows a GitHub repository page for 'linhvannguyen / PhDworks'. The repository name is 'PhDworks / isotropic /'. The commit history shows the following activity:

File	Commit Message	Time Ago
Bayesianfusion	Add files	28 days ago
comparison_plot	Add files	a month ago
datastats	Add files	a month ago
dictionarylearning	Remove some unused files	a month ago
regression	Update files	9 minutes ago
README.md	Update files	5 minutes ago

**PhD works - isotropic turbulence dataset**

This repos synthesizes all codes and data to reproduce our results in the thesis:  
Reconstruction of finely resolved velocity fields in turbulent flows from low resolution measurements

**Main parts**

The repos is comprised by the following main part

- Regression: linear and nonlinear regression; require [scikit-learn](#)
- Dictionary Learning: statistics of different learning approaches, couple dictionary learning by three post-processing techniques; require [SPAMS](#)(<http://spams-devel.gforge.inria.fr/>)
- NLM: Matlab and C code with openMP to speedup the computation
- Bayesian fusion: code to run all cases, with step to estimate the weights
- comparison\_plot: to compare all methods via NRMSE and plots
- datastats: statistics of the data

**License**

This project is licensed under the MIT License - see the [LICENSE.md](#) file for details

# References I

-  Bonnet, J. P., Cole, D. R., Delville, J., Glauser, M. N., and Ukeiley, L. S. (1994). Stochastic estimation and proper orthogonal decomposition: complementary techniques for identifying structure. *Experiments in fluids*, 17(5):307–314.
-  Buades, A., Coll, B., and Morel, J.-M. (2005). A review of image denoising algorithms, with a new one. *Multiscale Modeling & Simulation*, 4(2):490–530.
-  Corpetti, T., Mémin, É., and Pérez, P. (2002). Dense estimation of fluid flows. *IEEE Transactions on pattern analysis and machine intelligence*, 24(3):365–380.
-  Coudert, S., Foucaut, J. M., Kostas, J., Stanislas, M., Braud, P., Fourment, C., Delville, J., Tutkun, M., Mehdi, F., Johansson, P., and George, W. K. (2011). Double large field stereoscopic piv in a high reynolds number turbulent boundary layer. *Experiments in Fluids*, 50(1):1–12.

## References II

-  Dekou, R., Foucaut, J.-M., Roux, S., Stanislas, M., and Delville, J. (2016).  
Large scale organization of a near wall turbulent boundary layer.  
*International Journal of Heat and Fluid Flow.*
-  Durgesh, V. and Naughton, J. W. (2010).  
Multi-time-delay lse-pod complementary approach applied to unsteady high-reynolds-number near wake flow.  
*Experiments in fluids*, 49(3):571–583.
-  Hardie, R. C., Eismann, M. T., and Wilson, G. L. (2004).  
Map estimation for hyperspectral image resolution enhancement using an auxiliary sensor.  
*IEEE Transactions on Image Processing*, 13(9):1174–1184.
-  Papadakis, N., Mémin, É., Cuzol, A., and Gengembre, N. (2010).  
Data assimilation with the weighted ensemble kalman filter.  
*Tellus A*, 62(5):673–697.

## References III

-  Protter, M., Elad, M., Takeda, H., and Milanfar, P. (2009).  
Generalizing the nonlocal-means to super-resolution reconstruction.  
*Image Processing, IEEE Transactions on*, 18(1):36–51.
-  Schneiders, J. F., Dwight, R. P., and Scarano, F. (2014).  
Time-supersampling of 3d-piv measurements with vortex-in-cell simulation.  
*Experiments in Fluids*, 55(3):1–15.
-  Tu, J. H., Griffin, J., Hart, A., Rowley, C. W., Cattafesta, L. N., and Ukeiley, L. S. (2013).  
Integration of non-time-resolved piv and time-resolved velocity point sensors for dynamic estimation of velocity fields.  
*Experiments in fluids*, 54(2):1–20.
-  Yang, J., Wright, J., Huang, T. S., and Ma, Y. (2010).  
Image super-resolution via sparse representation.  
*IEEE transactions on image processing*, 19(11):2861–2873.

# Regression

**Parameter estimation** (regularization parameters, size of training data): *bias-variance trade-off, k-fold cross validation*

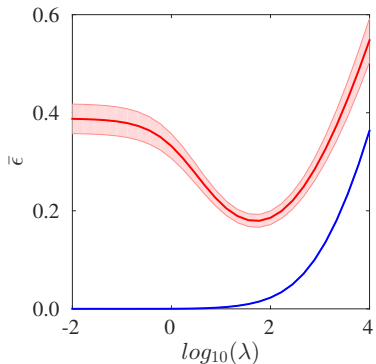


Figure: Validation curve

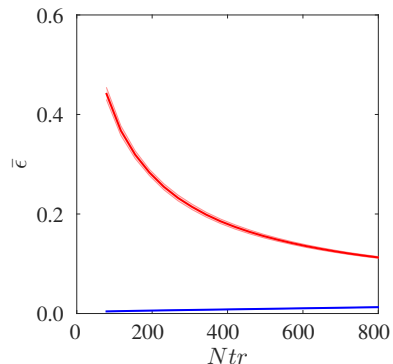


Figure: Learning curve

# Dictionary learning: error vs sparsity

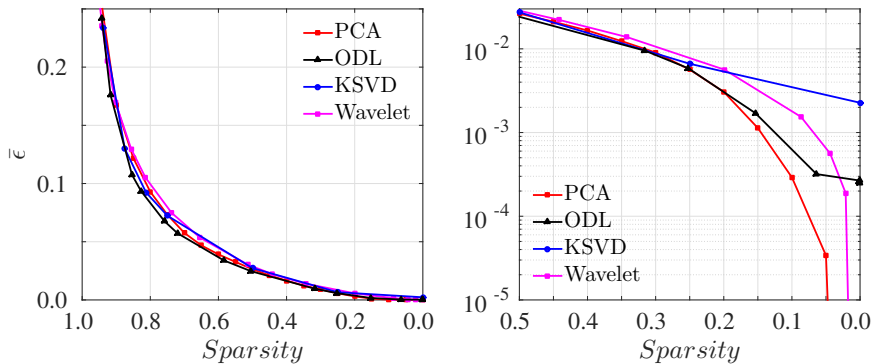


Figure: Sparsity vs error outside the training data

## MAP

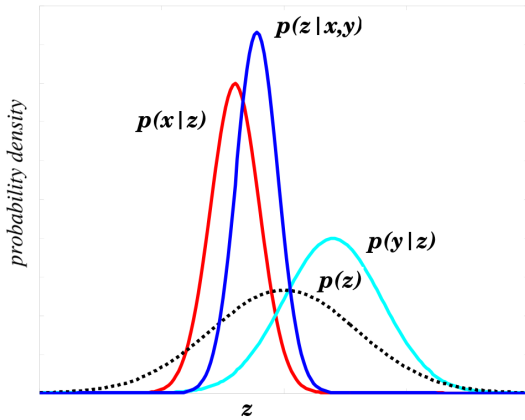


Figure: Sparsity vs error outside the training data

# Pdfs of velocity increments

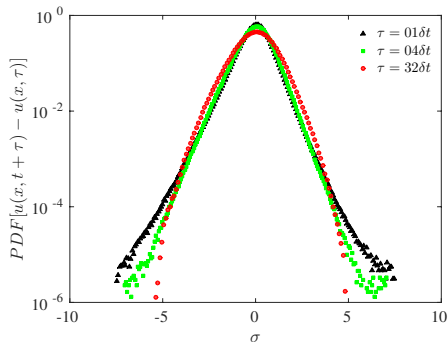
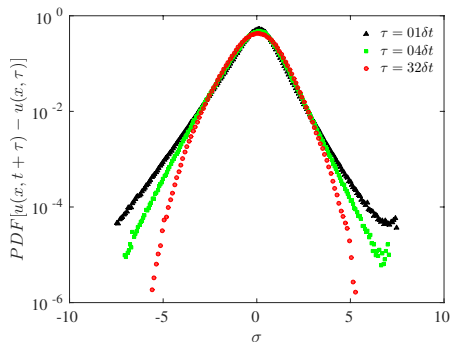


Figure: Probability density functions of velocity increments: reference and fusion

# Error map

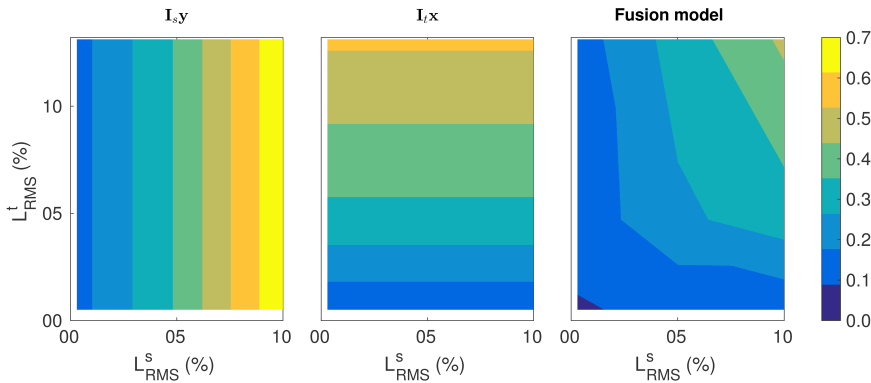


Figure: A map of errors as functions of energy losses

# NLM propagation

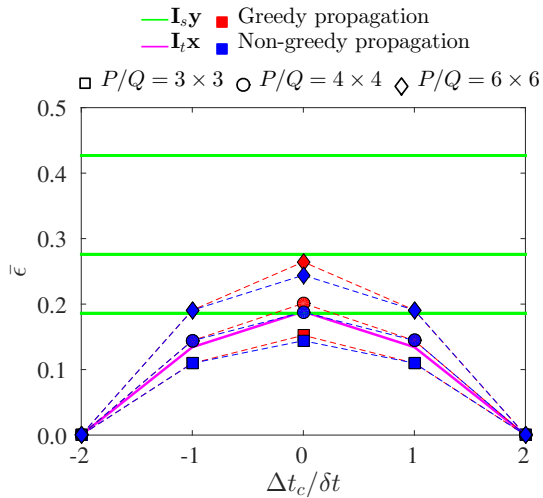


Figure: NRMSE when varying the sampling ratio in space

# NLM propagation

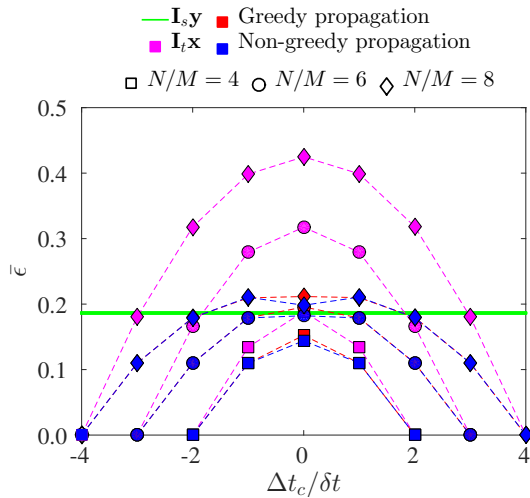


Figure: NRMSE when varying the sampling ratio in time